International Journal of Innovative
Computing, Information and Control
Volume **9**, Number **4**, April **2013**

ICIC International ©2013 ISSN 1349-4198
pp. 1627–1636

VIABLE HOPF BIFURCATION POINTS ELIMINATION WITH SVC FOR AN ELECTRICAL POWER SYSTEM FALLING INTO VOLTAGE COLLAPSE

Metin Varan, Yilmaz Uyaroglu and Mehmet Ali Yalcin

Department of Electrical and Electronics Engineering
Faculty of Engineering
Sakarya University
Esentepe-Serdivan, 54100, Turkey
{ mvaran; uyaroglu; yalcin }@sakarya.edu.tr

Received December 2011; revised April 2012

Abstract. *During last two decades many studies on power system stability have been reported that cascading voltage collapse events and formation of viable bifurcation points on Q-V curves are strictly related to each other. This paper presents an analytical control procedure to eliminate viable bifurcation points on Q-V curves that cause cascade voltage collapse events. After elimination procedure, stability margins of power system are extended to large loadability levels and viable bifurcation points on Q-V curves are changed by fewer viable ones that sustain system stability. During study, possible roles of small parameter changes of sample power system around bifurcation points have been traced over time series analysis, phase plane analysis and bifurcation diagrams. A wide collection of useful dynamic analysis procedures for the exploration of studied power system dynamics have been handled through the AUTO open-source algorithms.*
Keywords: Power system stability, Voltage collapse, Viable bifurcation points, Nonlinear system analysis, Small parameter changes

1. **Introduction.** A power system usually is expressed with nonlinear dynamic equations consisting of system parameters. Any change from the system parameters results in significant changes in the behaviour of the nonlinear dynamic system. System parameter change sometimes can lead to complex events. Such a system may show oscillatory behaviour as a result of instability in this system. Among several nonlinear mathematical theories [1], bifurcation analysis has been applied to investigate qualitatively the ways in which instabilities can take place in power system as well as how the system equilibrium points become unstable [2]. For example, after a load increment a stable operating point may become unstable and oscillations arise. This behaviour can be locally associated to a hopf bifurcation and, in general, bifurcation theory can be applied to understand mechanisms leading to nonlinear phenomena in these systems [3,4]. In this context, Kwatny and E. H. Abed demonstrate possible outcomes in the study of steady state stability of power systems in respect of dynamic (hopf) and static (saddle-node) bifurcations. On the other side, Dobson and Chiang have introduced a simple 3-bus power system model showing that the causes and effects between the load and generator create a saddle-node bifurcation. During such a situation, power system stability is highly dependent of the magnitude of reactive power demand. Bifurcation points on Q-V curves may crucially effect on the voltage on the load bus. Even small changes on reactive power demand cause sudden drops on load bus voltage called as voltage collapse phenomenon.

In this study, the 3-bus power system model is studied. This simple model has been widely studied using different sets of parameter values. This paper presents an analytical

control procedure to eliminate viable bifurcation points on Q-V curves that cause cascade voltage collapse events. After elimination procedure, stability margins of power system are extended to large loadability levels and viable bifurcation points on Q-V curves are changed by fewer viable ones that sustain system stability. Control strategy has been applied in context of demonstrating and then eliminating the change path of system stability loss, birth or death of oscillations, passage from periodic to chaotic solutions or vice versa.

This paper is organized as follows. In Section 2, complicated dynamical behavior of the nonlinear power system model is further investigated. In Section 3, design principles of static VAR compensator are explained. Section 4 considers definition of hopf bifurcation. Effects of designed control scheme on studied power system are discussed in after/before control comparison views in Section 5. A brief conclusion is presented in last section.

2. **System Model.** In this part of the study, as shown in Figure 1 after generating power, a power system consists of a powerful infinite busbar transmission line and nonlinear power loads. This model includes an infinite bus on the left that generates $V_0\angle 0$ constant voltage amplitude and the angle, a load bus and SVC device on the center, and a generator bus on the right that generates $V_m\angle\delta_m$ magnitude of voltage and angle. Detailed dynamics of generator buses are sketched into swing equations. Power system model also contains complex admittances of transmission line (Y_m and Y_0), an SVC and a load connected parallel with a capacitor. Load voltage and angle are assembled as $V\angle\delta$.

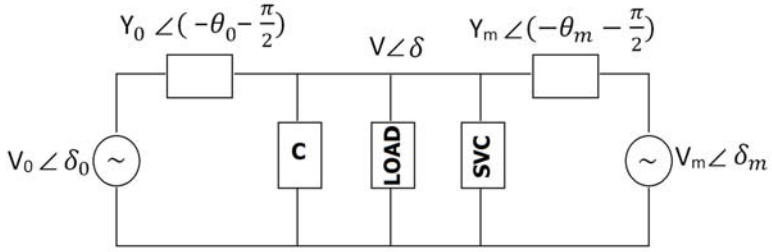

FIGURE 1. Schematic diagram of the 3-bus power system model with SVC

Swing equation dynamics of generator can be expressed as follows:

$$M\ddot{\delta}_m + D\dot{\delta}_m = P_m + V_m.V.Y_m.\sin(\delta - \delta_m - \theta_m) + V_m^2 Y_m \sin\theta_m \tag{1}$$

Here, M, D, P_m, θ_m are respectively, generator moment of inertia, damping coefficient, mechanical power generator and rotational angle. Load model contains a dynamic induction motor and a parallel connected constant P-Q load. Load includes a capacitor to maintain nominal and reasonable voltage amplitude. Load dynamics model can be expressed as follows:

$$P_d = P_0 + P_1 + K_{pw}\dot{\delta}_m \ + K_{pv}\left(V + T\dot{V}\right) \tag{2}$$

$$Q_d = Q_0 + Q_1 + K_{qw}\dot{\delta}_m \ + K_{qv}V + K_{qv2}V^2 \tag{3}$$

Here, $K_{pw}, K_{pv}, K_{qw}, K_{qv}, K_{qv2}$ expressions come from the induction motor dynamics and accepted as fixed. Furthermore, P_0, Q_0 and Q_1, P_1 represent active and reactive power demands for induction motor and P-Q load, respectively.

Active and reactive powers transmitted by the system to loads are:

$$P = -V_0^l V Y_0^l \sin(\delta + \theta_0^l) - V_m V Y_m \sin(\delta - \delta_m - \theta_m) + (Y_0^l \sin\theta_0^l + Y_m \sin\theta_m)V^2 \tag{4}$$

$$Q = V_0^l V Y_0^l \cos(\delta + \theta_0^l) + V_m V Y_m \cos(\delta - \delta_m + \theta_m) - (Y_0^l \cos\theta_0^l + Y_m \cos\theta_m)V^2 \tag{5}$$

By handling differential terms in the left side, the system dynamics are able to be described with following four ordinary differential equations:

$$\dot{\delta}_m = \omega_m \tag{6}$$

$$M\,\dot{\omega_m} = -D\omega_m + P_m + V_m V Y_m \sin(\delta - \delta_m - \theta_m) + V_m^2 Y_m \sin\theta_m \tag{7}$$

$$K_{qw}\,\dot{\delta} = -K_{qv2}V^2 - K_{qv}V + Q - Q_o + Q_{SVC} - Q_1 \tag{8}$$

$$\begin{aligned} TK_{qw}K_{pv}\dot{V} = {} & K_{pw}K_{qv2}V^2 + (K_{pw}K_{qv} - K_{qw}K_{pv})V \\ & + K_{pw}(Q_o - Qsvc + Q_1 - Q)K_{qw}(P_o + P_1 - P) \end{aligned} \tag{9}$$

State variables of given equations are generator voltage phase angle-θ_m, rotor speed-ω_m, load voltage phase angle-θ, load voltage-V.

Point-indices over variables show the t-derivatives. During the analysis, Q_1 reactive power demand value is chosen as bifurcation parameter.

3. **Static VAR Compensator Model.** Studied SVC scheme includes of a fixed capacitor connected in parallel with a thyristor controlled reactor. The effective reactance of the controlled reactor is a function of the firing angle of the thyristor. The SVC function, therefore, is equivalent to providing a continuously controlled shunt susceptance to the system [5-7]. The SVC studied in this paper is modeled as a first order linear differential equation

$$\dot{B} = \frac{1}{T_{SVC}}(K_{SVC}u - B); \quad B_{\min} \le B \le B_{\max} \tag{10}$$

Here, B is the susceptance of the SVC, K_{SVC} is the SVC gain, T_{SVC} is the SVC time constant and u is the control input to the SVC (see Figure 2). The node that voltage needs to be controlled should be connected with SVC. Generally SVC devices are connected at the middle of a transmission line or at a load bus. In this paper, the SVC is connected paralelly with the load bus as sketched into Figure 1.

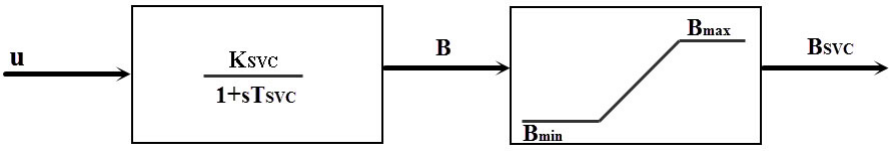

FIGURE 2. Schematic diagram of static feedback controlled SVC

In static state feedback, the SVC input is given by:

$$u = k_s(V_L - V_0) \tag{11}$$

Here, V_0 is the reference voltage means targeted operating voltage, and V_L is load bus voltage that SVC connected. Substituting Equation (10) into Equation (11), then following expression can be written

$$\dot{B} = \frac{1}{T_{SVC}}(K_{SVC}k_s(V_L - V_0) - B), \quad B_{\min} \le B \le B_{\max} \tag{12}$$

The actual effect of the variable susceptance introduced to the system by the SVC is modeled as an additional reactive power Q_{SVC} that is added to the load reactive power.

$$Q_{SVC} = BV_L^2 \tag{13}$$

With SVC control, the reactive power supplied by the SVC to the power system is given by (13) which is added to Q_1 in Equations (3) and (4).

4. **Hopf Bifurcation Analysis.** Consider a power system dynamic model which is represented by an autonomous differential equation of the form:

$$\dot{x} = F(z, p) \tag{14}$$

where x is the n-dimensional state vector and p is a parameter. If the parameter is varied, the corresponding state vector x and the eigenvalues of the Jacobian df/dx evaluated on this path change accordingly. Near an equilibrium point the left hand side term $\dot{x}$ becomes zero:

$$F(x, p) = 0 \tag{15}$$

Equation (15) specifies the position of the equilibrium point x as a function of p. The power system state on the surface defined by Equation (15) is asymptotically stable if the eigenvalues of the Jacobian have negative real parts at that point. One of the ways the system can reach a critical state is if a real eigenvalue becomes zero or a pair of complex conjugate eigenvalues crosses the imaginary axis.

Bifurcation theory is interested in how solutions $x(p)$ branch as p varies [8-10]. These changes, when they occur, are called bifurcations and the parameter values at which a bifurcation happens are called bifurcation values. Equation (15) specifies the position of the equilibrium point x as a function of p. One type bifurcation is a saddle-node bifurcation. The saddle-node bifurcation occurs the disappearance of system equilibrium as parameters change slowly [11].

For example consider the quadratic equation:

$$x^2 - p = 0 \tag{16}$$

The variable x represents the system state and p represents a system parameter. When p is negative there are two equilibrium solutions $x_0 = \sqrt{-p}$ and $x_0 = -\sqrt{-p}$.

If p increases to zero then both equilibria are at the double rout $x = 0$. If p increases further and becomes positive, there are no equilibrium solutions. The bifurcation occurs at p_0 at the critical case separating the case of two real solutions from no real solutions.

The power system state on the surface is asymptotically stable if the eigenvalues of the jacobian have negative real parts at that point. One way the system can reach a critical state is if a real eigenvalue becomes zero or a pair of complex conjugate eigenvalues crosses the imaginary axis. When a complex conjugate pair of eigenvalues crosses the imaginary axis and moves into the right half plane the system may start oscillating with small amplitude. This phenomenon is described by hopf bifurcation theory [8,12,13].

5. **Studied Power System Model.** Power system parameters are given below.

Load parameter values:

$$K_{pw} = 0.4,\ Q_o = 1.2,\ K_{pv} = 0.3,\ P_1 = 0,\ K_{qw} = -0.03,$$
$$T = 8.5,\ K_{qv} = -2.8,\ P_o = 0.6,\ K_{qv2} = 2.1.$$

Network and generator parameter values:

$$Y_o = 10,\ P_m = 1,\ M = 0.25,\ V_o = 1,\ D = 0.05,$$
$$Y_o' = 8,\ V_o' = -2.5,\ \theta_m = -8,\ \theta_o = -12,\ V_m = 1.05.$$

Here, the angle values in radian, the time in milliseconds, and the other parameters in the unit value (per unit: pu) are quoted.

With initial conditions of the system will be shown by

$$\dot{I}_o = (\delta_{mo}, \omega_{mo}, \delta_o, V_o, Q_{1o})$$

Initial conditions parameters are respectively

δ_m: *Generator angle*

ω_m: *Generator angular velocity*
δ: *Load angle*
V: *Load voltage*
Q_1: *Reactive power demand for PQ load*

And, initial conditions parameters are taken $\dot{I}_o = (0.4, 0.02, 0.1, 0.95, 9.879)$, respectively. In this paper, bifurcation points are identified through combined assesment of eigenvalues. In Figure 3, bifurcation points are shown by HB, SHB, SNB and UHB abbreviations.

For HB point $\dot{I}_o = (\delta_{mo}, \omega_{mo}, \delta_o, V_o, Q_{1o})$ is (0.3244, 0.0000, 0.1240, 1.0526, 10.1215) and "first lyapunov coefficient" is $-14.352645\text{e}+001$.

For UHB point $\dot{I}_o = (\delta_{mo}, \omega_{mo}, \delta_o, V_o, Q_{1o})$ is (0.3359, 0.0000, 0.1320, 0.9317, 10.1862) and "first lyapunov coefficient" is $5.455\text{e}-001$.

For SHB point $\dot{I}_o = (\delta_{mo}, \omega_{mo}, \delta_o, V_o, Q_{1o})$ is (0.3378, 0.0000, 0.1375, 0.9727, 10.2587) and "first lyapunov coefficient" is $-7.388638\text{e}-001$.

For SNB point $\dot{I}_o = (\delta_{mo}, \omega_{mo}, \delta_o, V_o, Q_{1o})$ is (0.3785, 0.0000, 0.1456, 0.9659, 10.450) and "first lyapunov coefficient" is $-1.388638\text{e}-003$.

Figure 4 depicts the changes of relevant eigenvalues of HB, SHB, SNB and UHB at equilibrium points. The eigenvalues are calculated by substituting (HB, SHB,SNB and UHB) values of the system equilibrium points into values of state variables in the Jacobian matrix [5]. There are four eigenvalues for each equilibrium point because of system's representation by four first order state equations. At the $Q1 = 9.80$ and $Q1 = 10.00$ values, the eigenvalues are $(e1 = -138,662,\ e2,3 = -0.42 \pm 3.873i,\ e1 = -14,12)$ and $(e1 = -127,435,\ e2,3 = -0.34 \pm 3.538i,\ e1 = -9,54)$, respectively. It is clear that eigenvalues are far from unstability margin. At $Q1 = 10.12$ (HB), the eigenvalues are $(e1 = -117,755,\ e2,3 = -0.0034 \pm 2.857i,\ e1 = -7,65)$. Necessary condition for hopf bifurcation is satisfied by the presence of complex conjugate eigenvalues with real part Re[2] 0 and Re[3] 0. Real part of conjugate eigenvalues at HB point is very close to stability margins borders. Unstable/supercritical hopf bifurcation point and stable/subcritical hopf bifurcation are detected at $Q1 = 10.20$ and $Q1 = 10.27$ values, respectively. The eigenvalues at $Q1 = 10.20$ are $(e1 = -95,735,\ e2,3 = +0.00039 \pm 2.436i,\ e1 = -4,19)$. Real part of conjugate eigenvalues at UHB point are out of stability margins borders.

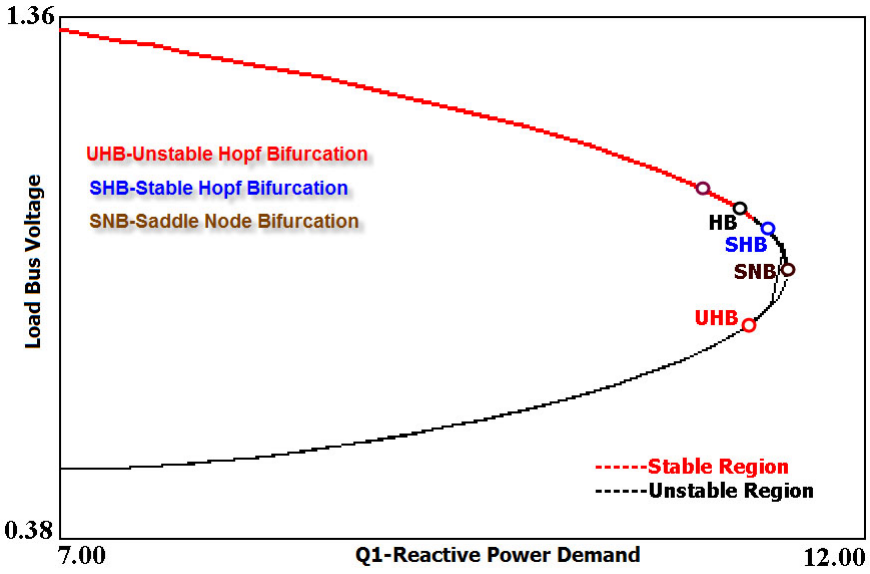

FIGURE 3. Bifurcation diagram before installing SVC

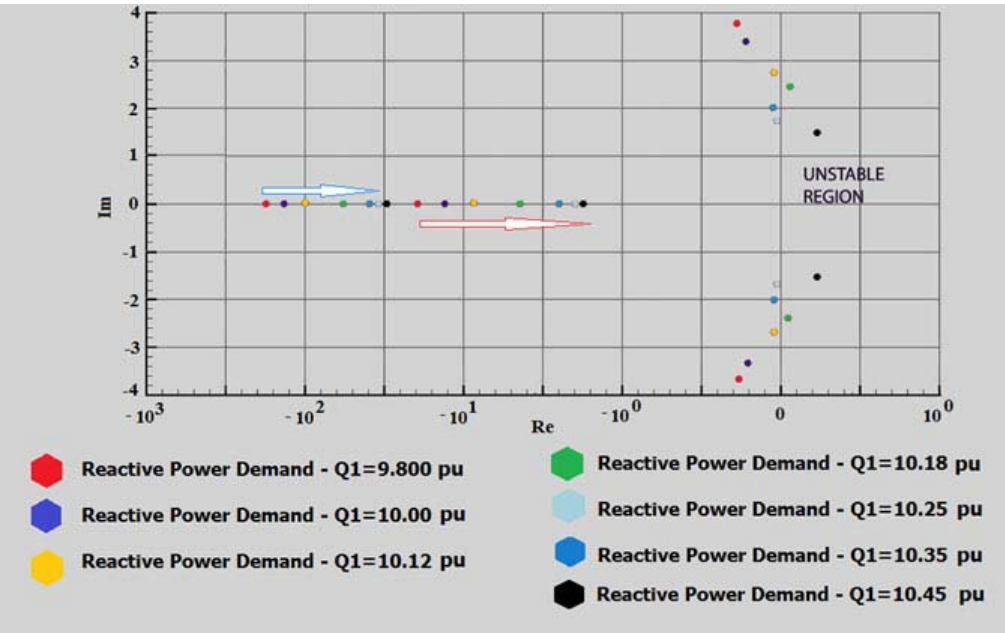

FIGURE 4. Changes of eigenvalues for power system equilibrium Point before installing SVC

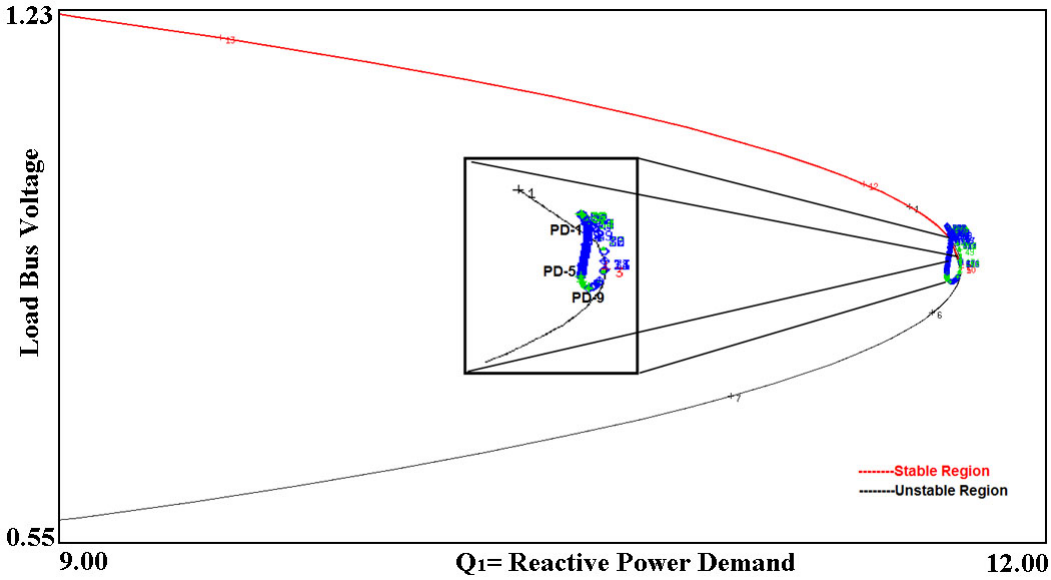

FIGURE 5. Period doubling branches in bifurcation diagram before installing SVC

However, the other system dynamics remain into stability margins. As seen in Figure 5 supercritical hopf point at $Q1 = 10.20$ value has family of unstable periodic solutions that undergo a period doubling cascade starting from PDB 1 to PDB 3.

In Figure 6(a), Figure 6(c) and Figure 7(a), formation of PDB 1, PDB 2 and PDB 3 is demonstrated on load bus voltage and load bus angle phase portraits, respectively. Figure 6(b), Figure 6(d) and Figure 7(b) show time series of load bus voltage at PDB 1, PDB 2 and PDB 3. With a further increase in Q_1, the equilibrium point undergoes SHB which falls again into the stability margins. At SHB point, system starts to increase number of doubling cycle from PD3 to PD9. With a further increase in $Q1$, the equilibrium point

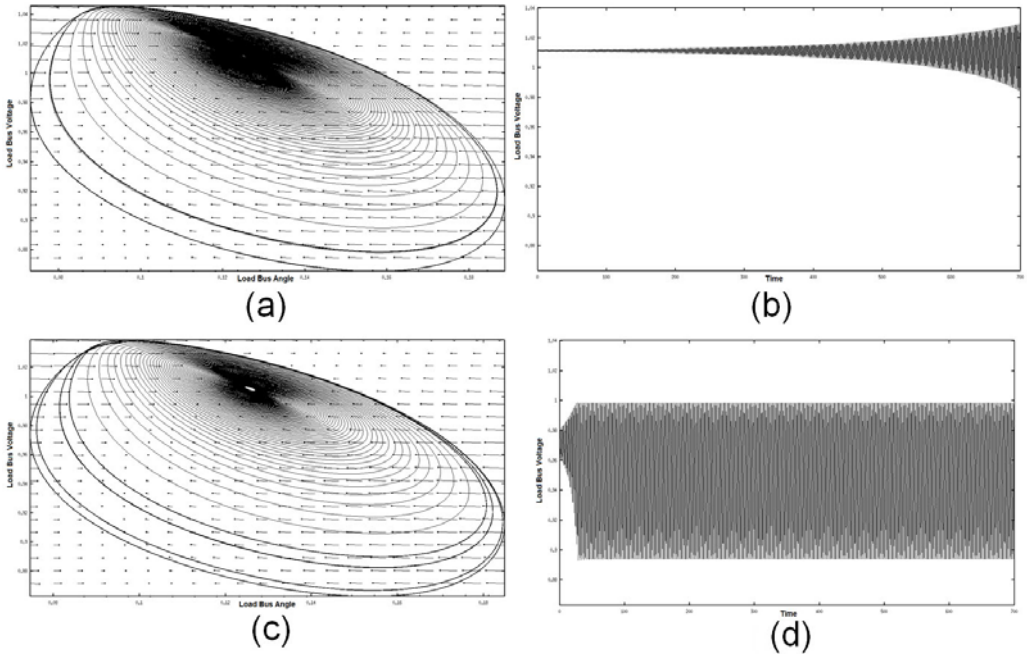

FIGURE 6. Phase portraits of load bus voltage-load bus angle and time series of load bus voltage at given period doubling bifurcation points before installing SVC

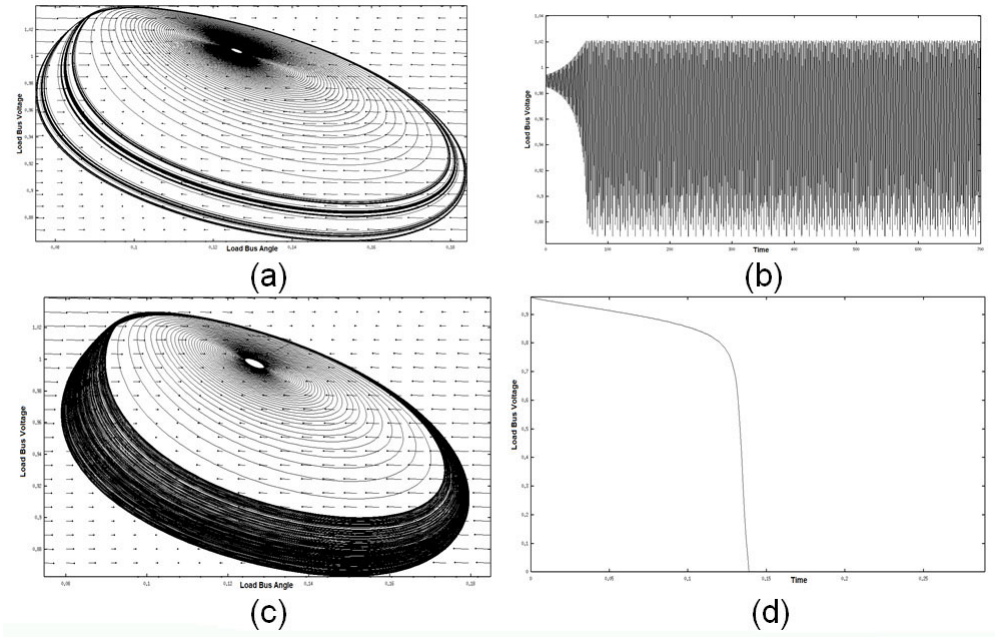

FIGURE 7. Phase portrait of load bus voltage-load bus angle and time series of load bus voltage at given period doubling bifurcation point before installing SVC

undergoes SNB point accumulating a critical value of $Q1 = 10.40$. The creation of chaotic attractor for $Q_1 = 10.40$ is shown in Figure 7(c). The Lyapunov exponent in this case found to be 0.187, which confirms chaotic nature. After this point a small increase in system parameter results into voltage collapse event as sketched into Figure 7(d).

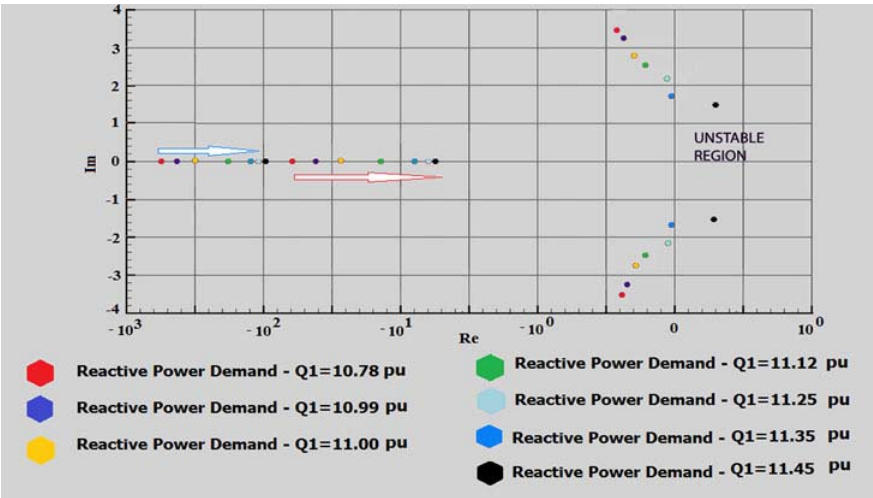

FIGURE 8. Changes of eigenvalues for power system equilibrium point after installing SVC

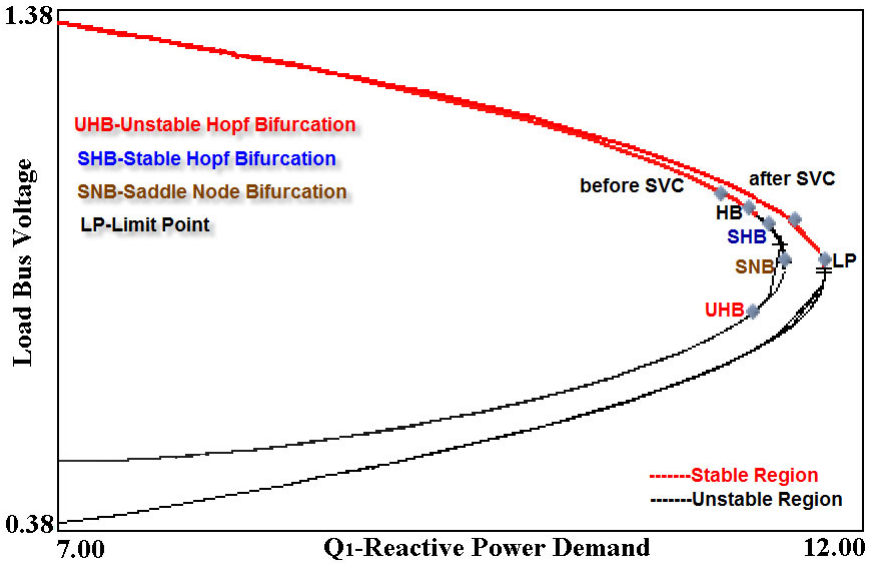

FIGURE 9. Bifurcation diagram before/after installing SVC

The bifurcation diagram of the studied power system after installing SVC using static state feedback of the controller gain k_s at -0.90 value is depicted in Figure 8 and Figure 9. The constants of installed SVC are $T_{SVC} = 0.0145$ s and $K_{SVC} = 5$. When comparing after and before installation of SVC scenario, Figure 8 and Figure 9 demonstrate positive effects of designed static feedback controller procudure. As sketched on Figure 8, proposed SVC scheme extends stability margins of power system from 10.45 pu reactive power demand to 11.45 pu loadability levels. Also, unstable eigenvalues are transfered into stability margins.

As seen bifurcation diagram sketched in Figure 9, it is clear that designed SVC extends stability margins of power system to larger loadability levels and alters viable bifurcation points on Q-V curve by fewer viable one (LP-Limit Point) that sustain system stability.

Designed SVC scheme also delays voltage collapse event even in larger reactive power demand values as shown in Figure 10.

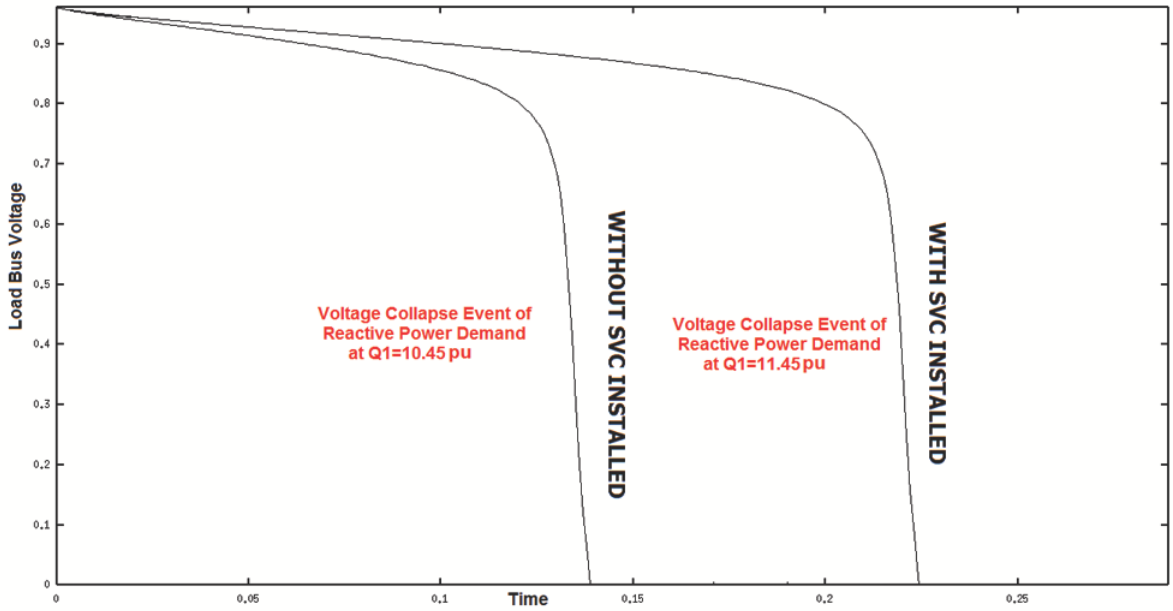

FIGURE 10. Load bus voltage changes over time before/after installing SVC

6. **Conclusion.** This paper presents an analytical control procedure to eliminate viable bifurcation points on Q-V curves that cause cascade voltage collapse events. During study, possible roles of small parameter changes of sample power system around bifurcation points have been traced over time series analysis, phase plane analysis and bifurcation diagrams. As shown in mentioned diagrams it is clear that designed SVC extends stability margins of power system to larger loadability levels and alters viable bifurcation points on Q-V curve by fewer viable one (LP-Limit Point) that sustain system stability.

Acknowledgment. This work is supported in part by the Scientific Research Support Program Fund in Sakarya University with grant-number: 2011-50-02-008.

REFERENCES

[1] I. A. Hiskens, Analysis tools for power systems – Contending with nonlinearities, *Proc. of IEEE*, vol.83, pp.1573-1587, 1995.
[2] A. Medina and M. A. Martinez, Application of bifurcation theory to assess nonlinear oscillations produced by AC electric arc furnaces, *IEEE Trans. on Power Delivery*, vol.20, no.2, pp.801-806, 2005.
[3] G. Revel, D. M. Alanso and J. L. Moila, Bifurcation theory applied to the analysis of power systems, *Revista De La Union Math. Argentina*, vol.49, no.1, pp.1-4, 2008.
[4] R. Wang and J. Huang, Effects of hard limits on bifurcation, chaos and stability, *Acta Mathematicae Applicatae Sinica*, vol.20, no.3, pp.441-456, 2004.
[5] W. Marszalek and Z. Trzaska, Singular hopf bifurcations in DAE models of power systems, *Energy and Power Engineering*, vol.3, no.1, pp.1-8, 2011.
[6] Q. Du, Z. Su and S. Li, Some design and simulation of SMVSC for hopf bifurcation in power systems, *Energy and Power Engineering*, vol.3, no.1, pp.24-28, 2011.
[7] P. Javanbakht, M. Noroozian, M. Abedi and G. B. Gharehpet, The enhancement of transient stability of a wind farm in a weak network using SVC and OLTC, *International Journal of Distributed Energy Resources*, vol.6, no.4, pp.325-341, 2010.
[8] H. S. Strogatz, *Nonlinear Dynamics and Chaos*, Cambridge-Perseus Publishing, 2000.
[9] J. D. Crawford, Introduction to bifurcation theory, *Reviews of Modern Physics*, vol.4, no.1, pp.991-992, 1991.

[10] P. K. Satpathy, D. Das and P. B. D. Gupta, A fuzzy approach to handle parameter uncertainitiesin Hopf bifurcation analysis of power systems, *Int. Journal Elect. Power Energy Syst.*, vol.26, no.7, pp.527-534, 2004.

[11] D. Wei, X. Luo and B. Zhang, Noise-induced voltage collapse in power systems, *China Physics Letters*, vol.29, no.3, pp.1-5, 2012.

[12] N. Mithulananthan, C. A. Canizares, J. Reeve and J. R. Graham, Comparison of PSS, SVC and STATCOM controllers for damping power system oscillations, *IEEE Trans. on Power Syst.*, vol.18, no.2, pp.786-790, 2003.

[13] Y. Ma, H. Wen, X. Zhou, J. Li, H. Yang and X. Zhou, Multi-parameter static bifurcation analysis of wind power system based on dynamic model, *Advanced Science Letters*, vol.4, no.4, pp.1792-1795, 2011.